

A microtube viscometer with a thermostat

Z. H. Silber-Li, Y. P. Tan, P. F. Weng

586

Abstract The viscometer presented in this paper is suitable for measuring the viscosity of liquids in micro-litre quantities. It consists of a micro-flow experimental system with a thermostat. Using the measurements of the flow rates and pressure drops of a liquid passing through a microtube, the liquid's viscosity can be calculated from the Hagen-Poiseuille theory. After calibration, the viscometer was used to measure viscosities of deionized water and ethyl alcohol at temperatures ranging from 0 to 40 °C. For both test liquids, the relative deviation of the measured values from those quoted in the literature (obtained using other viscometers) was less than 2.6%. The relative uncertainty of the experimental system was reduced to $\pm 1.8\%$ using the relative measuring method. Due to the micro-scale of the test section, only a micro-litre quantity of liquid is needed for a test; this is a potential advantage for measurement of bio-liquid viscosities.

1 Introduction

Viscosity is one of the important physical properties of liquids. Since the viscosity of a liquid can vary according to other physical properties such as temperature and pressure, it is perhaps more accurately called the *dynamic* viscosity. The accurate measurement of viscosity is important for many major industries, such as the petroleum and chemical industries, and metallurgy. In these industries, being able to perform viscosity measurements

is essential for effectively controlling the production process, in order to maintain product quality and to make the process as economic as possible. Recently in medicine, the viscosity measurement of blood and of other biological liquids has become a new diagnostic method for detecting some potentially fatal diseases, such as cancers, tumours and cardiovascular diseases. In physical chemistry, hydrodynamics, and other scientific fields, viscosity is a very important physical quantity in relation to understanding the nature of a liquid and its fluid flow behaviour.

Liquid viscosity is caused by molecular attraction. It depends on the liquid's physical behaviour, pressure conditions and the environmental temperature. The variation of viscosity with temperature is often described by an equation given by Van Wazer et al. (1963):

$$\mu = Be^{\frac{E}{RT}} \quad (1)$$

where B is a constant, R is the universal gas constant, and T is the absolute temperature (in K). E is the apparent activation energy of the liquid, which represents the energy used by a molecule in moving from one place to another; it relates to the molecule's structure, the length of molecular chains, and temperature conditions.

The viscosity of a particular liquid under standard experimental conditions can often be found in reference books or other reference literature. However, actual experimental densities and concentrations of liquids are usually different to standard conditions, so it is often necessary to measure the viscosity for the experimental conditions actually used.

Capillary, rotating, and falling-ball viscometers have most generally been used for liquid viscosity measurements. Capillary viscometers are the most commonly-used type for the measurement of Newtonian liquid viscosity. They have a simple construction and are convenient to use. Falling-ball viscometers, which make use of Stokes Law, are mainly used for low viscosity substances. Rotating viscometers are used for the measurement of non-Newtonian liquids, due to the steady rotation movement (Van Wazer et al. 1963).

In some situations, such as in a clinical laboratory, the amount of liquid available for measurement is quite small. But with current viscometers, even the simplest capillary viscometer, the diameter of the capillary is of the order of a millimetre, and more than 1 ml of liquid is used for each test. Large-scale viscometers also have restricted use, since thermostatic baths are commonly used for adjusting temperature but their implementation is usually complicated and expensive for a wide range of test temperatures.

Received: 20 November 2002 / Accepted: 25 September 2003
Published online: 4 March 2004
© Springer-Verlag 2004

Z. H. Silber-Li (✉), Y. P. Tan
LNM, Institute of Mechanics,
Chinese Academy of Sciences,
15, Bei Si Huan Xi Lu, 100080 Beijing, China
E-mail: lili@lnm.imech.ac.cn

Y. P. Tan, P. F. Weng
Shanghai Institute of Applied Mathematics and Mechanics,
Shanghai University, 200072
Shanghai, China

The authors express their sincere gratitude to senior engineer Liu Zongyuan, engineer Liu Bin, and doctoral candidate Cui Haihang, for their help in designing and debugging. Thanks are also due to National Foundation Research (Item G1999033106), Chinese Academy of Sciences (Major Innovation Project KJCX2-SW-L2), and National Natural Science Foundation of China (10272107) for their support of this research.

Therefore, a viscometer of a small scale is often most desirable.

The field of microtechnology has become important in recent years (Gad-el-Hak 1999), and it provides a possible new approach for the miniaturization of viscometers. In this paper, we use the liquid microflow to measure liquid viscosity and construct a thermostat that uses the Peltier effect. A driving flow under pressure is used instead of the gravity flow used in a capillary viscometer. Using measured values of pressure and flow rates, the liquid's viscosity can be calculated (see Sect. 2). We will discuss the principles of the experimental set-up and the uncertainties in the measurement in Sect. 3. Calibration will be discussed in Sect. 4, where we discuss viscosity tests of two liquids, and compare our experimental results with the values obtained using the classic methods (see Sect. 5.1). In order to improve the measurement accuracy, a relative measurement method is proposed in Sect. 5.2, and a comparison is made between our viscometer and commercial ones in Sect. 5.3.

2

Basic theory

According to fluid mechanics, the incompressible and laminar flow driven by pressure through a tube with a constant diameter is called Hagen-Poiseuille flow, and its motion equation is:

$$\nabla_x P = \mu \nabla^2 u \quad (2)$$

where P is the pressure, μ the fluid viscosity, and u the axial velocity along the x direction. If d and ℓ are the diameter and the length of the tube, respectively, μ can be expressed as follow:

$$\mu = \frac{\pi d^4}{128 Q \ell} \Delta P \quad (3)$$

where Q is the volumetric flux, and ΔP is the pressure drop at the two ends of the tube. This formula shows that the viscosity coefficient is related to ΔP , Q and the tube's geometric sizes. According to the experiments of Sharp et al. (2001), when the tube diameter varies from 200 μm to 50 μm , the fluid flow still behaves as a Hagen-Poiseuille flow. From the recent experiments of Li et al. (2002), for simple liquids, even if the tube's diameter is as small as 20 μm , the flow behaviour still agrees with the H-P law. Because of this, the test section of our viscometer is a micro-tube with diameter of 20 μm .

3

Experimental set-up

The viscometer presented in this paper appears similar to the experimental set-up for microflow attached to a thermostat to adjust the temperature. This microflow experimental set-up has been commonly used in many microflow experiments (Pfahler et al. 1990; Jiang et al. 1995; Mala and Li 1999; Li and Cui 2002). The set-up is shown in Fig. 1a. It consists of three main parts: the driving source unit, the test section, and the flux measurement unit. The driving source may be a liquid pump (Pfahler et al. 1990; Mala and Li 1999) or a high pressure

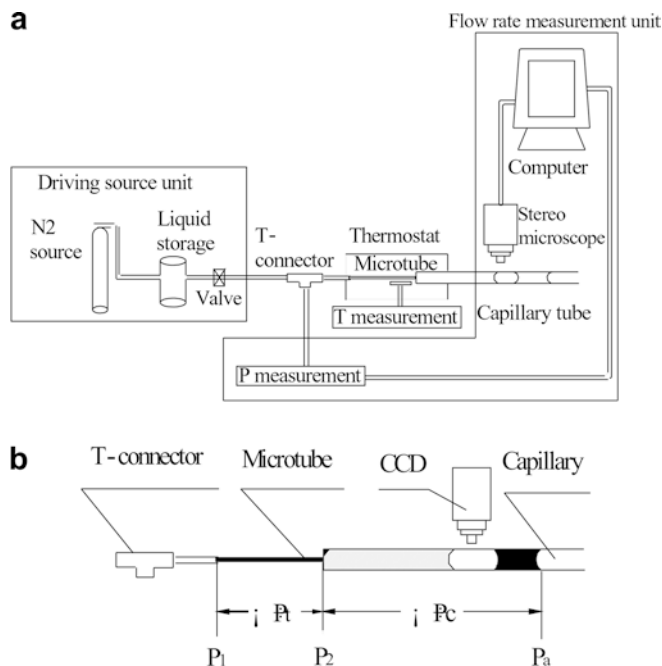


Fig. 1 a Schematic of the viscometer set-up, b detailed drawing of pressure drop and flow rate measurement

source of N_2 (Jiang et al. 1995). Our experimental set-up uses the latter. The liquid in storage, driven by pressure, passes through a T-connector into the test section. The test section includes a microtube of 20 μm in diameter, a thermostat, and pressure and temperature measurement apparatus. A pressure transducer is connected to the T-connector and indicates the inlet pressure of the microtube at position P_1 (see Fig. 1b). The microtube passes through the thermostat, in which the test temperature can be adjusted in the range of 0~45 $^\circ\text{C}$. A thermocouple installed inside the thermostat indicates the temperature of the test liquid (the construction of the thermostat will be discussed in detail in Sect. 4). The flux measurement unit includes a capillary 1~2 mm in diameter and a CCD connected to a stereomicroscope and a computer. The other end of the microtube is connected to the capillary by glue. The other end of the capillary is open to the atmosphere, with pressure P_a . The measurements of the pressure drop and flow rate are described as follow:

1. *Measurement of pressure drop ΔP .* $\Delta P = \Delta P_t + \Delta P_c$, where ΔP_t is the pressure drop in the microtube and ΔP_c is that in the capillary. From Fig. 1b, we know $\Delta P_t = P_1 - P_2$ and $\Delta P_c = P_2 - P_a$. From Eq. 3, ΔP is inversely proportional to the fourth power of the tube's diameter. As the microtube's diameter is 20 μm , which is 1/50 of the capillary's diameter (1 mm), then $\Delta P_t \gg \Delta P_c$. Therefore we have $\Delta P \approx \Delta P_t$ and $\Delta P_t \approx P_1 - P_a$.
2. *Measurement of flow rate Q .* The displacement method is used to measure Q . The test liquid passing through the microtube is gathered in the capillary. The end surface of the liquid's column is scanned by the CCD system. The flow rate through the capillary can be calculated by the formula:

$$Q = \frac{AS}{t} = \frac{\pi D^2 S}{4t} \quad (4)$$

where A and D are the sectional area and the diameter of the capillary, respectively. S is the displacement of the liquid's surface in the capillary and t is the interval time of the measurement. Because of continuity, the flow rate Q in the microtube is the same as that in the capillary.

3.1 Experimental uncertainty

Based on Eqs. 3 and 4, the measured viscosity μ_{exp} can be expressed as:

$$\mu_{\text{exp}} = \frac{d^4}{32D^2 \ell} \frac{\Delta P}{S/t} = f(d, D, \ell, S, t, \Delta P) \quad (5)$$

According to the theory of error analyses (Holman 1984), the uncertainty of an experimental system is related to the individual uncertainty of all related quantities, which in turn depends directly on their measurement methods. Therefore, μ_{exp} depends on the geometric sizes (microtube's diameter d and length ℓ , capillary's diameter D) and the physical parameters (displacement S , time t , pressure P). A Scanning Electronic Microscope (SEM) with a resolution of 0.1 μm was used to measure the microtube's diameter. A ruler with a resolution of 0.01 mm was used to measure the length ℓ . The diameter of the capillary was measured by a tool microscope with a resolution of 0.005 mm. The flow rate was measured by the displacement method (see Sect. 3). A ruler under the CCD, with a resolution of 0.025 mm, was used to measure the distance, and a watch with a resolution of 100 ms was used to measure the time. The pressure transducer used in the experiments was calibrated to a precision of 0.3%. Based on the instruments and methods employed in our experiments, the uncertainties of the measurement parameters are shown in Table 1.

From Eq. 5, the relative uncertainty of the experimental system with respect to the mean measured viscosity $u_B/\bar{\mu}_{\text{exp}}$ can be calculated as:

$$\begin{aligned} \frac{u_B}{\bar{\mu}_{\text{exp}}} &= \pm \sqrt{\sum_{i=1}^6 \left(\frac{\partial \ln f}{\partial x_i} \right)^2 dx_i^2} \\ &= \pm \sqrt{\left(\frac{4}{d}\right)^2 u_d^2 + \left(\frac{2}{D}\right)^2 u_D^2 + \left(\frac{1}{S}\right)^2 u_S^2 + \left(\frac{1}{\ell}\right)^2 u_\ell^2 + \left(\frac{1}{t}\right)^2 u_t^2 + \left(\frac{1}{P}\right)^2 u_P^2} \end{aligned} \quad (6)$$

where u_i indicates the uncertainty in the measurement of property i . Based on the data in Table 1, Eq. 6 is evaluated

Table 1. Experimental parameters and uncertainties

Parameters	Symbols (units)	Values and uncertainties	
		Deionized water	Ethyl alcohol
Diameter of microtube	d (μm)	19.9 \pm 0.1	21.3 \pm 0.1
Length of microtube	L (mm)	52.47 \pm 0.01	48.70 \pm 0.01
Diameter of capillary	D (mm)	0.977 \pm 0.005	1.064 \pm 0.005
Distance of displacement	S (mm)	3.000 \pm 0.025	3.000 \pm 0.025
Time interval	t (s)	600.0 \pm 0.1	600.0 \pm 0.1
Pressure drop	P (kPa)	200.0 \pm 0.6	100 \pm 0.3

as $\pm 2.4\%$ for water and $\pm 2.3\%$ for alcohol. From Eq. 6, the principal uncertainty clearly comes from the geometric sizes, such as the diameters of the microtube and capillary. This encourages us to propose a relative method, which will be discussed in Sect. 5.2.

3.2 Other factors that influence the experimental error

1. The entrance effect was also considered. The Reynolds number of flow is less than 2.2 and the microtube's diameter is 20 μm , which is much smaller than its length of 5 cm. Therefore, the entrance effect can be omitted
2. Vapour may appear on the liquid's surface while measuring flow rates. To avoid the effect of the vapour from the surface of the liquid's column, we put a gas bubble in the column before the test. The displacement S is measured from the downstream interface of this bubble (see Fig. 1b)
3. The uncertainty of the temperature measurement in the experiments is not considered in Eq. 6. From the reference data (Weast and Astle 1982), the viscosity of water varies 1.9~3.3% per $^\circ\text{C}$ over the range 0–40 $^\circ\text{C}$. If the thermostat's accuracy is about 0.3 $^\circ\text{C}$ (see Sect. 4.2), an uncertainty of 1.0% should be added to the result of Eq. 6. Considering that water viscosity varies more with temperature than for other liquids, this error value should be safe to use for all test liquids.

4 Thermostat

4.1 Working principle

As shown in Fig. 2, the thermostat consisted of a metal coverlet, a liquid storage, a semiconductor cooler (or heater), a thermocouple, and a microtube shell. A sheet of thermal insulation material covered the coverlet. Since the coverlet is made of metal, the heat transfers from the source to the storage and to the shell rapidly. The semiconductor cooler (or heater) makes use of the Peltier effect of thermoelectricity: when an electric current flows across the junction between two dissimilar metals, it leads to a release or absorption of heat, proportional to the current. Therefore, in principle, the passage of the current across the junction of two dissimilar conductors can be used for

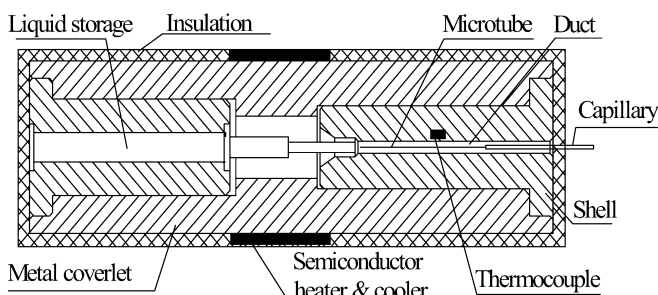


Fig. 2. Sketch of thermostat

cooling as well as heating, depending upon the direction of the current (Quinn 1983). Semiconductors are used here for large Peltier coefficients. The function of the semiconductor cooler/heater was controlled by the feedback signal, which comes from comparing the thermocouple readings with the target value. The microtube penetrated through the duct of the shell, which is 3 mm in diameter. A thermocouple was installed at the inner wall of the duct to measure the temperature near the microtube. A calibration was performed to measure the difference between the temperature reading and the actual temperature of liquids in the microtube.

4.2 Calibration

As mentioned above, the test liquid's temperature T_L was measured by a digital thermocouple, with a reading T_W of uncertainty of ± 0.1 °C. A calibration was made to measure the difference between T_W and T_L . Due to the small diameter of only 20 μm of the microtube, it was difficult to measure T_L directly. But there are two factors that may affect T_L : the liquid temperature T_H in the storage upstream of the microtube, and the temperature gradient along the axial direction of the microtube in the shell. Therefore, the calibration was carried out in two steps: first, by comparing T_W and T_H ; second, by analysing and measuring the temperature gradient along the axial direction of the microtube in the shell.

4.2.1

Measuring the temperature T_H in the liquid storage

The diameter of the liquid storage was 8.3 mm (Fig. 2). We placed a mercury thermometer with an measuring uncertainty of ± 0.05 °C inside the liquid storage filled with deionized water, and sealed the storage with some heat-insulated material. The mercury thermometer gave the reading T_H . The target temperature T_0 was established at the beginning of the test. If T_0 was higher than the room temperature, the heating process of the thermostat started. Otherwise, the cooling process was activated. After several periods of heating/cooling, T_W approached T_0 gradually and remained within a range of $\Delta T (=T_W - T_0)$. In the cooling process of the calibration, ΔT varied between 0.2~0.5 °C, the fluctuation period Δt was 80~130 s; in the heating process, ΔT varied between 0.2~0.7 °C and Δt was 70~160 s. The average values of T_W and T_H were taken over one period. Based on the data from several periods, T_W and T_H can be expressed as $T_W = \bar{T}_W \pm u_{TW} = \bar{T}_W \pm 0.1$ °C and $T_H = \bar{T}_H \pm u_{TH} = \bar{T}_H \pm 0.05$ °C. Here, \bar{T}_W and \bar{T}_H are the arithmetic means, while u_{TW} and u_{TH} are the uncertainties of the thermometer measurements. From the results of calibration (Fig. 3), the deviation between \bar{T}_W and \bar{T}_H ranges from 0.05–0.2 °C, so the experimental uncertainty is ± 0.2 °C. Therefore, the thermocouple's reading T_W well represents the liquid's temperature T_H in the storage.

4.2.2

Evaluating the temperature gradient in the shell

As shown in Fig. 2, heat is transmitted in the coverlet from the semiconductor to the shell. The conducting distance is around 10 cm. The coverlet is made of duralumin.

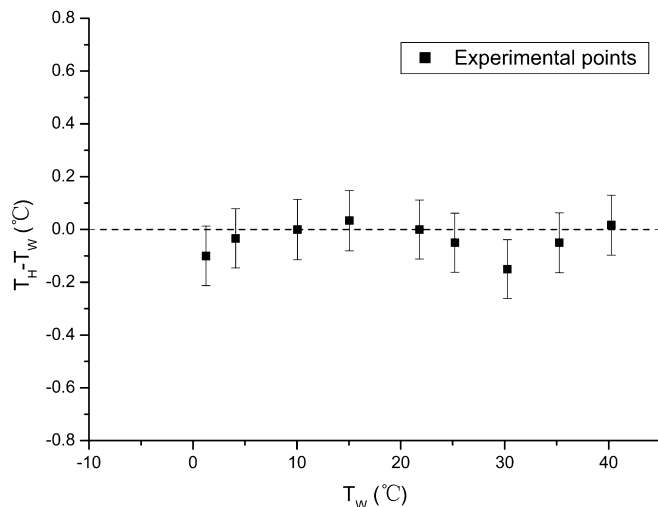


Fig. 3. Deviation between liquid's temperature in the storage T_H and thermocouple's reading T_W at different T_W

Supposing that the semiconductor is a point source, the thermal transfer equation can be expressed as (Landau and Lifshitz 1998):

$$\frac{\partial T}{\partial t} = \chi \nabla^2 T \quad (7)$$

where χ is the thermometric conduction ($\chi = k/\rho C_p$), ρ is the material's density, C_p is the specific heat, and k is the thermal conductivity of the material. For evaluating the temperature gradient in x , we consider a one-dimensional model: the heat source is located at the origin of x , the shell is parallel to x and the downstream boundary is infinite. In this case, Eq. 7 can be simplified to:

$$\frac{\partial T}{\partial t} = \chi \frac{\partial^2 T}{\partial x^2} \quad (8)$$

Based on the boundary conditions and zero initial temperature, the solution to this is:

$$\frac{\partial T}{\partial x} = -\frac{1}{k} \int_0^t \frac{xq}{2\sqrt{\pi\chi t^3}} e^{-\frac{x^2}{4\chi t}} dt \quad (9)$$

where q is the heat per square metre, and t is the observing time. Considering the power of the source (15 V and 6A, $5 \times 5 \text{ cm}^2$) and the transformation efficiency from electric to thermal energy (30%), q may be evaluated to be $1.2 \times 10^4 \text{ W/m}^2$. For aluminium, k is 164 W/m K, ρ is 2787 kg/m³ and C_p is 833 J/kg K (Kreith and Bohn 2001). After five seconds, the temperature gradient is close to 0.05 °C/cm at $x=5$ cm. Therefore, the temperature difference along the microtube is close to 0.4 °C for the length of 5 cm. It should be noted that several simplifications have been made in the mathematical model here: an instantaneous heat source replaces a discontinuous one in tests; the infinite boundary condition is used for the protecting boundary. However, such a simple model is useful for evaluating the order of magnitude as a first step. The measurement of the temperature distribution in the duct is described in the next section.

4.2.3

Measuring the temperature T_G in the shell

A thermocouple was located in the duct of the shell without a microtube in it. The end of the duct was sealed with some heat-insulating material. The thermocouple was used to measure the gas temperature T_G in the duct. The room temperature was 20 °C in the test and the target temperatures were 5, 15, 30 and 40 °C. The measurements were made at three positions X_1 , X_2 and X_3 along the shell. The distances from the origin were 22, 43 and 68 mm, respectively (Fig. 4). At each position, the test was repeated more than three times. The measured values for T_G are presented as $T_G = \bar{T}_G \pm u_{T_G} = \bar{T}_G \pm 0.1$ °C. The uncertainties in the thermometer measurements were constant, so the mean values are presented in Fig. 5 without showing uncertainties. The difference between T_W and T_G increases as T_0 moves away from the room temperature. Therefore, the temperature gradient between X_1 and X_3 becomes important. However, even for $T_0 = 5$ °C to 40 °C, the temperature gradient between X_1 and X_3 is smaller than 0.1 °C/cm and the variation of $T_W - T_G$ is within ± 0.5 °C. A mean value of $T_W - T_G$ is ± 0.3 °C.

On the basis of the calibration results, it can be seen that the thermocouple's readings T_W reflect the liquid temperature T_L well in the microtube, with an uncertainty of ± 0.3 °C. If the semiconductor heater/cooler is controlled by an electrical source, which can modulate the voltage exactly, the temperature fluctuation range will be well limited and the uncertainty will be further reduced.

5

Results

5.1

Tests with liquids

Using this viscometer, we tested two liquids: deionized water and ethyl alcohol. The sample water for measuring the viscosity must be pure. Deionized water was obtained via the Milli-Q water purification system (Millipore Company), and it had an electrical conductivity of about $2.73 \mu\text{S cm}^{-1}$. The room temperature was about 20 °C. The test temperature range varied from 1.6 to 40.3 °C and the pressure drop was adjusted to 0.1 MPa. The concentration of ethyl alcohol was 99.8%. The test temperature varied from 0 to 39.9 °C and the pressure drop was 0.2 MPa. The

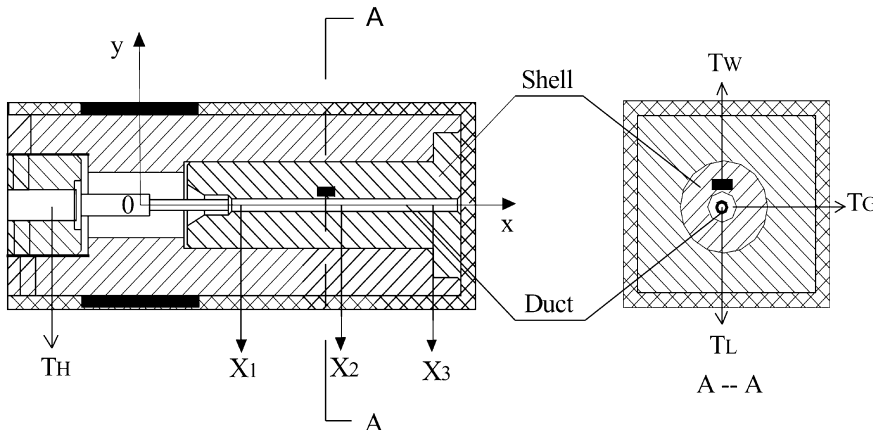


Fig. 4. Scheme of measuring positions

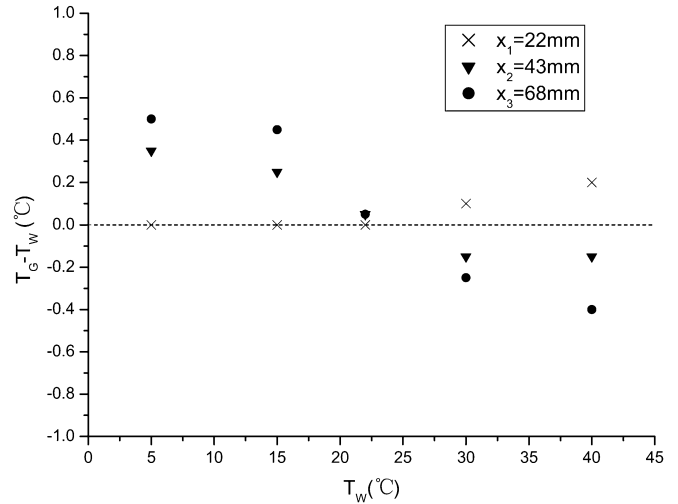


Fig. 5. Distribution of the difference between T_W and T_G vs T_W at different positions: X_1 (×'s), X_2 (inverted triangles), X_3 (circles)

measurement included two steps: in the heating process, the target temperature T_0 was 25, 30, 35, 40 °C; in the cooling process, T_0 was 15, 10, 5, 1 °C. For each T_0 , it took 30 minutes to stabilize. The thermocouple readings T_W were recorded during the fluctuation periods. If the differences between mean readings in successive periods were greater than 0.5%, the measurements were made all over again. The results were treated with the theory of error analysis (Holman 1984). The arithmetic mean value of the measured viscosity at point j is expressed as:

$$\bar{\mu}_{\text{exp}j} = \frac{1}{N} \sum_i^N \mu_{\text{exp}i} \quad (10)$$

where N is the measurement number. The standard deviation (RMS deviation) of the measured viscosity can be calculated as:

$$u_{A_j} = \pm \zeta \left[\frac{\sum_i^N (\mu_{\text{exp}i} - \bar{\mu}_{\text{exp}j})^2}{N - 1} \right]^{1/2} \quad (11)$$

Here ζ is a coefficient related to N ($3 \leq N \leq 5$, $\zeta = 1.2 \sim 2.5$; $N > 5$, $\zeta = 1$). u_{A_j} represents the random error of

the measured values. Another part of error due to the experimental system is expressed by u_{Bj} . It can be calculated using Eq. 6 in Sect. 3.1. Therefore, the experimental uncertainty $u_{\mu j}$ is expressed as:

$$u_{\mu j} = \pm \sqrt{u_{Aj}^2 + u_{Bj}^2} \tag{12}$$

The measured viscosity μ_{exp} is expressed as:

$$\mu_{exp j} = \bar{\mu}_{exp j} \pm u_{\mu j} \tag{13}$$

The measured viscosities were compared with those values quoted in the literature (μ_{th} , obtained from the Handbook by Weast and Astle 1982). A relative deviation η_j is defined as:

$$\eta_j = \frac{|\bar{\mu}_{exp j} - \mu_{thj}|}{\mu_{thj}} \times 100\% \tag{14}$$

Based on the experimental results, the arithmetic mean value of the measured viscosity for water $\bar{\mu}_{exp}$ ranges from 0.67 to 1.73 mPa s (Fig. 6). The standard deviation u_{Aj} is $\pm(2.0\sim 5.4)\times 10^{-3}$ mPa s, which is much smaller than u_{Bj} calculated from Eq. 6 in Sect. 3.1. Therefore, the relative uncertainty of experiment to mean value of the measured viscosity $u_{\mu j}/\bar{\mu}_{exp j}$ is less than $\pm 3.4\%$, and the experimental uncertainties range from $\pm(2.3\sim 5.9)\times 10^{-2}$ mPa s. The relative deviation η_j is less than 2.6%. For alcohol, $\bar{\mu}_{exp}$ ranges from 0.85 to 1.79 mPa s with experimental uncertainties of $\pm(2.8\sim 5.9)\times 10^{-2}$ mPa s, corresponding to a relative uncertainty of the experimental system of $\pm 3.3\%$. The relative deviation η_j is less than 1.4%.

5.2 The relative method

From Eq. 5 in Sect. 3.1, the measured viscosity is a function of several parameters which influence the experimental arithmetic mean values and uncertainties. Among them,

the geometric sizes show dominant effects. However, these quantities (microtube's diameter d and length ℓ , capillary's diameter D) are fixed once the tubes and capillaries are installed in the system. By means of the relative method, a constant C can be introduced to eliminate these effects. Equation 5 can be rewritten by substitution of Eq. 4 as:

$$\mu = C\Delta P \left(\frac{t}{S}\right) \tag{15}$$

where S and t are the displacement and the interval time of the liquid's surface in the capillary. Supposing that μ_{20} is the data at 20 °C obtained from the Handbook, C can be determined from the test:

$$C = \mu_{20} \frac{S_{20}}{t_{20}\Delta P} \tag{16}$$

Combining Eqs. 15 and 16, we can see that the measured viscosity relates only to S , t (ΔP is constant in the tests). In this way, the relative uncertainty of the experimental system to the mean measured values for water $u_B/\bar{\mu}_{exp j}$ is reduced to $\pm 0.8\%$, which is much smaller than that for the absolute method of $\pm 2.4\%$. The relative experimental uncertainty $u_{\mu j}/\bar{\mu}_{exp j}$ is reduced to $\pm 1.8\%$, and the relative deviation η_j becomes less than 1.5%. For alcohol, the relative experimental uncertainty is reduced from $\pm 3.3\%$ to $\pm 1.8\%$. Therefore the accuracy of experiments obviously increases (Fig. 7).

5.3 Comparison with commercial viscometers

As we mentioned in the *Introduction*, capillary, rotating and falling-ball viscometers are commonly used for liquid viscosity measurements. The viscometer presented in this paper is similar to a capillary viscometer, but a microtube is used as the test section in place of the capillary. For the experiments, the flow rate for water was less than 22 nl s⁻¹ and the measuring time was less than 800 seconds. In addition to a waiting time of only 30 minutes before the

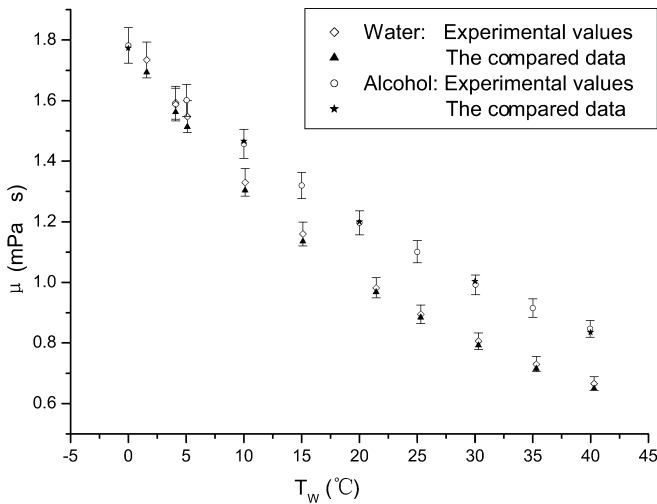


Fig. 6. Comparison between the measured viscosity treated by the absolute method and the literature values. For water: experimental values (diamonds), the compared values (triangles); for alcohol, experimental values (circles), the compared values (stars)

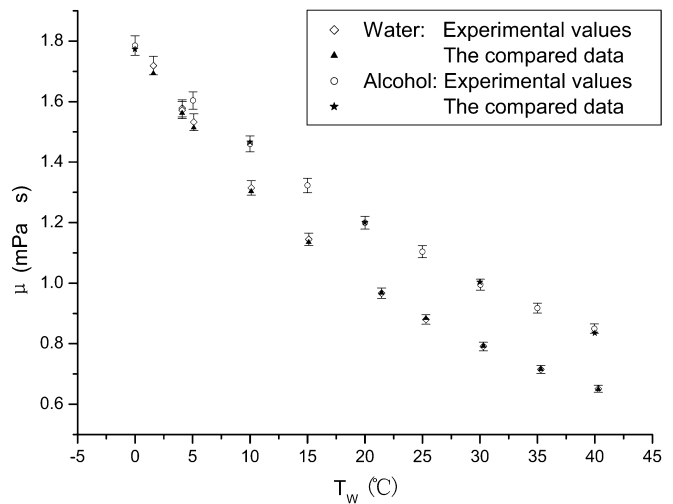


Fig. 7. Comparison between the measured viscosity treated by the relative method and the literature values. For water: experimental values (diamonds), the compared values (triangles); for alcohol, experimental values (circles), the compared values (stars)

Table 2. A brief comparison of the microtube viscometer and commercial viscometers

Name	Type	Measured viscosity (mPa s)	Liquid volume (ml)	T (°C)	Test time (min)	Heating method and price	Refs.
Microtube viscometer	Capillary	<10	0.06	0~40	<30	Semiconductor ~200US\$	-
Cannon-Manning Semi-Micro Extra Low Change viscometer	-	-	0.5	-	-	Thermostatic bath ~2500US\$	(1)
Pinkevitch Grabner Minivis II	- Falling sphere	<20 <20*	1-10 0.4	20-40* 0~100	10 3~10	- Thermoelectric regulation	- (2)

(1) <http://203.147.186.54/html/Cannon>; (2) <http://www.petrolab.com/fp-mv.htm>; * evaluated values

test, it needs less than 60 μl of liquid for each test point. A brief comparison with current viscometers is presented in Table 2; only viscometers that use small liquid volumes are selected.

From Table 2, we may make the following remarks:

1. The test liquid volume of the microtube viscometer is less than that of any other commercial viscometer.
2. A thermostat based on the Peltier effect is used in our viscometer, which takes a longer time to measure the temperature. If the electric power of the semiconductor can be regulated according to the target temperature, the test time will be reduced. However, its miniaturisation is a big advantage, as compared with the thermostatic bath used in other viscometers.
3. If the thermostat's power or driving pressure were to be increased, the microtube viscometer could be used for a wider temperature range and for liquids with higher viscosity.

6 Conclusions

The viscometer presented in this paper is suitable for measuring the viscosity of microlitre volumes of liquid. It is based on a micro-flow experimental system and a thermostat. By measuring the flow rate and pressure drop through a microtube of 20 μm diameter under different temperatures, the liquid's viscosity coefficients can be calculated based on Hagen-Poiseuille theory. The main results are as follows:

1. Two examples of the application of the viscometer were given: deionized water and ethyl alcohol. The test temperature range was from 0 to 40 °C, and the viscosity coefficients varied over the range 0.6~1.8 mPa s. In the experiment, pressure drops were regulated at 0.1~0.2 MPa and the Reynolds number was less than 2.2. The experimental results showed that the measured viscosities agree well with the data in the literature (obtained from the Handbook). The relative deviation of measured values from the cited data was less than

2.6% for water and 1.4% for alcohol. The relative experimental uncertainty was $\pm 3.4\%$ for water and $\pm 3.3\%$ for alcohol, which is mainly due to the uncertainty in the geometric sizes of the microtubes. With the relative measuring method, the relative experimental uncertainty for both liquids can be reduced to $\pm 1.8\%$.

2. The microtube viscometer has potential advantages over current viscometers due to its smaller sample volume and the thermostat of the semiconductor. With the development of MEMS techniques, the viscometer can be further miniaturised.

References

- Gad-el-Hak M (1999) The fluid mechanics of microdevices—the freeman scholar lecture. *J of Fluids Engineering* 121:5-33
- Holman JP (1984) *Experimental methods for engineers*, 5th edn. McGraw-Hill, New York, p 549
- Jiang XN, Zhou ZY, Yao J, Li Y, Ye XY (1995) Micro-fluid flow in microchannel. Digest of technical papers from Transducers '95/Eurosensors IX, Stockholm, Sweden, 25-29 June 1995, Vol 2, pp 317-320
- Kreith F, Bohn S (2001) *Principles of heat transfer*, 6th edn. Brooks Cole, Florence, KY, p 700
- Landau LD, Lifshitz EM (1998) *Fluid mechanics*, 2nd edn. Butterworth Heinemann, Oxford, UK, p 539
- Li ZH, Cui HH (2002) Proceedings of experiments about liquid flow through micro-tubes. *Int J Nonlinear Sci* 3(3/4):577-580
- Li ZH, Zhou XB, Zhu SN (2002) Flow characteristics of non-polar organic with small molecules in a microchannel (in Chinese). *ACTA Mech Sinica* 34:432-438
- Mala MG, Li DQ (1999) Flow characteristics of water in microtubes. *Int J Heat Fluid Fl* 20:142-148
- Pfahler J, Harley J, Bau H, Zemel J (1990) Liquid transport in micron and submicron channels. *Sensor and Actuators*, A21-A23:431-434
- Quinn TJ (1983) *Temperature*. Academic, London
- Sharp KV, Adrian RJ, Santiago JG, Molho JI (2001) Liquid flows in microchannels. In: Gad-el-Hak M (ed) *MEMS Handbook*. CRC, Boca Raton, FL, 6:1-38
- Van Wazer JR, Lyons JW, Kim KY, Colwell RE (1963) *Viscosity and flow measurement*. Wiley, New York, p 406
- Weast RC, Astle MJ (1983) *CRC Handbook of Chemistry and Physics*, 63rd edn. CRC, Boca Raton, FL, pp F-38-F-46